Matching domain-wall configuration and spin-orbit torques for efficient domain-wall motion

A. V. Khvalkovskiy,[1] V. Cros,[2,*] D. Apalkov,[1] V. Nikitin,[1] M. Krounbi,[1] K. A. Zvezdin,[3] A. Anane,[2] J. Grollier,[2] and A. Fert[2]

[1]*Samsung Electronics, Semiconductor R&D (Grandis), San Jose, CA 95134, USA*

[2]*Unité Mixte de Physique CNRS/Thales and Université Paris Sud, Palaiseau, France*

[3]*A.M. Prokhorov General Physics Institute, Russian Academy of Sciences and Moscow Institute of Physics and Technology, 141700,*

Institutskii, 9, Dolgoprudny, Moscow Region, Russia

In our numerical study, we identify the best conditions for efficient domain-wall motion by spin-orbit torques originating from the spin Hall effect or Rashba effect. We demonstrate that the effect depends critically on the domain-wall configuration, the current injection scheme, and the symmetry of the spin-orbit torque. The best identified configuration corresponds to a Néel wall driven by the spin Hall effect in a narrow strip with perpendicular magnetic anisotropy. In this case, the domain-wall velocity can be a factor of 10 larger than that for the conventional current-in-plane spin-transfer torque.

PACS number(s): 75.70.Ak, 75.60.Ch, 75.78.Fg

The fundamental concepts of spintronics are based on the generation, manipulation, and detection of spin polarized currents. In the past two decades it has led to the development of a new generation of magnetic sensors, and notably read heads of hard disks and of nonvolatile magnetic memories (MRAMs) that are expected to supplant semiconductor based memory devices. In classical spintronics, one generally creates a spin current by passing a charge current through a thin ferromagnetic layer, whose magnetization direction can be controlled by an external applied field or more efficiently by spin-transfer torques. Recently an alternative way has emerged to control the magnetization configuration of a ferromagnetic layer that is based on current-induced spin-orbit (SO) torques, namely, the spin Hall effects (SHEs)[1] and the Rashba effect.[2] Such SO torques are expected for magnetic stripes adjacent to a nonmagnetic conductive layer with strong spin-orbit interactions (SO layer).[3] The exploitation of these SO effects opens up alluring possibilities for the development of a novel generation of highly reliable and low energy spintronic devices. In particular, several experiments have already demonstrated the great interest of the SHE and/or Rashba effects in metallic nanostructures to switch the magnetization[4–8] of a single nanomagnet or to drive magnetization dynamics.[9,10]

In this Rapid Communication, we discuss the relevance of these SO effects for obtaining the most efficient manipulation of domain walls (DWs) in magnetic nanoribbons. We use micromagnetic simulations to explore the impact of SO torques on the DW motion for both in-plane and perpendicularly magnetized magnetic layers. We consider different DW types, i.e., Bloch wall (BW), Néel wall (NW) in perpendicularly magnetized materials, or head-to-head DW (HTH), and relative orientations of the electron flow and the orientation of the magnetic stripe. We find that some of these geometrical configurations are particularly promising for fast DW motion induced by spin-orbit torques with small current densities.

We first introduce the two types of SO torques under investigation here. As for the spin Hall effect, an interfacial spin accumulation is created through the imbalance of the deflections of spin up and spin down electrons away from the electric field direction in a nonmagnetic layer.[1] The resulting transverse pure spin current can be injected into an adjacent magnetic layer in order to exert a spin-transfer torque and manipulate the magnetization. The spin Hall angle Φ_H is the parameter characterizing the maximum yield for the conversion of a longitudinal charge current density into a transverse spin current density:

$$j_s = \Phi_H j_c/e, \tag{1}$$

where j_c is the charge current and e the electron charge. After the initial predictions by Dyakonov and Perel, the first experimental observations in pure metals[11] or semiconductors[9,12] have confirmed, either by optical means or magnetotransport measurements, the existence of spin currents associated with SHE. However, the deduced spin Hall angles had relatively modest values. Interestingly, very recently, large values of the SH angle have been reported in metals and alloys, up to $\Phi_H = 0.11$–0.15 in Ta,[6] $\Phi_H = 0.24$ in Cu doped with Bi impurities,[13] and $\Phi_H = 0.33$ in W,[14] which shifts the interest in SHE from an exotic transport phenomena to an effective driving force for magnetization manipulation.

The second spin-orbit-related phenomena is the Rasbha effect,[2,3] which is induced by the electric field gradient due to a symmetry breaking at a surface or interface, typically a system composed of SO-metal/ferromagnetic metal/oxide. It results in a coupling by exchange between spin and momentum in surface or interface states expressed by the Rashba Hamiltonian,

$$\hat{H}_R = \alpha_R \vec{s} \cdot (\vec{k} \times \hat{e}_z), \tag{2}$$

where $\vec{s}$ is the spin, α_R is the Rashba parameter, $\hbar\vec{k}$ the electron's momentum, and $\hat{e}_z$ a unit vector perpendicular to the surface or interface. Experimentally, Rashba spin-orbit splittings have been measured by angle-resolved photoemission spectroscopy (ARPES) only for a few metallic or semiconductor interfaces states and the extracted Rashba parameter remains small with α_R values in the range of 10^{-11} eV m. Remarkably, a very large value has been observed at Bi/Ag interfaces, $\alpha_R = 3 \times 10^{-9}$ eV m, making Bi-based systems particularly attractive for spin-orbit driven control of the magnetization.[15] In the presence of the Rashba interaction, the charge current flowing in a magnetic thin layer in a
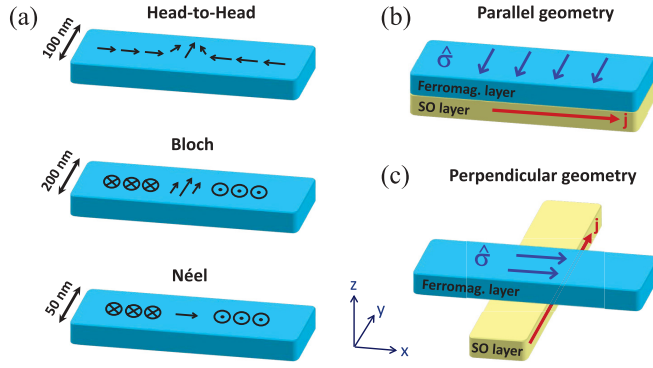
FIG. 1. (Color online) (a) Schematic view of the three different DW types that have been considered, i.e., head-to-head DW in an in-plane magnetized strip, Bloch or Néel DW in an out-of-plane magnetized strip. (b) Parallel geometry in which the ferromagnetic layer (F) is parallel to the spin-orbit (SO) layer on the whole length of the strip. (c) Perpendicular geometry for which the SO strip is perpendicular to the F strip.

direction parallel to the interface generates a spin accumulation that can interact by exchange with the magnetic moment of the adjacent magnetic material. Recent experiments by Miron *et al.* suggest that equivalent Rashba fields of $\approx$3–10 kOe can be created by this interaction.[4,5] In addition to this effective field, the Rashba-induced spin accumulation can give rise to an additional term of spin-transfer torque, called later the "indirect Rashba effect" (IRE). This new term has been predicted to arise from the spin diffusion inside the magnetic layer.[16] We note that the two types of Rashba terms have also been derived by a quantum kinetic theory of the current-induced torques in Rashba systems.[17] The symmetry and the influence of these new contributions among the spin-orbit transfer torques will be discussed later.

The main objective of this work is to investigate the effect of SHE and Rashba torques acting on three different types of DWs that are head-to-head (HTH) DWs in magnetic nanostrips with in-plane magnetization, Bloch wall, and Néel DWs in out-of-plane magnetized nanostrips [see Fig. 1(a)]. In our simulations, we have used structures that are bilayers consisting of (i) a ferromagnetic nanostrip called (F) and (ii) a nanostrip made of a material with large spin-orbit (SO) coupling. In order to address all possible symmetries, we have considered two different sample geometries. First, the parallel geometry [see Fig. 1(b)] corresponds to the most common geometry studied in the experiments for which both the SO layer and the magnetic material are stacked in the same nanostrip. The second case corresponds to perpendicular nanostrips [see Fig 1(c)] for which the different SO torques will be active only at the intersection of the two layers.

From now, we aim at analyzing the influence of the torques generated either by spin currents resulting from a combination of SHE and IRE or by the coupling of the magnetization of the F layer with the Rashba field. It is also important to specify that the direction of the spin accumulation in the SO layer depends on the direction of the charge current that flows along the magnetic wire axis in the parallel geometry [Fig. 1(b)] and perpendicular to the magnetic wire in perpendicular geometry [Fig. 1(c)]. Note that we use here the same approach

as the one we proposed to highlight the crucial advantage of perpendicular spin current injection to generate large DW velocities considering classical spin-transfer torques.[18] Finally, the two possible symmetries for the spin-orbit torques per unit moment that are acting on the local magnetization correspond to the following expressions for the time derivative of the unit vector $\hat{m}$ along the magnetization axis:

$$\vec{\tau}_1 = -\gamma \tau_1 (\hat{m} \times \hat{\sigma} \times \hat{m}), \tag{3}$$

$$\vec{\tau}_2 = -\gamma \tau_2 (\hat{m} \times \hat{\sigma}), \tag{4}$$

where $\hat{\sigma} = \hat{j} \times \hat{z}$, $\hat{j}$, and $\hat{z}$ are unit vectors in the current and out-of-plane directions and γ is the gyromagnetic ratio. The torque $\vec{\tau}_1$ in Eq. (3) presents a symmetry similar to the classical Slonczewski torque (SLT) or in-plane torque generated by the injected spin current density j. As far as the role of the spin Hall effect is considered, we suppose for simplicity that this spin current density has its optimal value, i.e., $\Phi_H j_c/e$, as expressed in Eq. (1). The resulting torque magnitude τ_1 (in unit moment) can be written as

$$\tau_1^{\text{SHE}} = \frac{\hbar \Phi_H j_c}{2e M_S t_F}, \tag{5}$$

where t_F is the thickness of the ferromagnetic layer (F) and M_S its saturation magnetization. The second torque $\vec{\tau}_2$ in Eq. (4) has the same symmetry as the classical fieldlike torque (FLT) or also called the perpendicular torque. It is now generally admitted that this second torque remains very weak in metallic systems,[18] whereas very large perpendicular torques are predicted in magnetic tunnel junctions[19] and confirmed experimentally with large DW velocities induced by spin torques with perpendicular injection.[20] Consequently, as the system we study here is composed of metallic layers, one gets

$$\tau_2^{\text{SHE}} \ll \tau_1^{\text{SHE}}. \tag{6}$$

If we now consider that the torque is due to the Rashba effect (RE), one generally considers only the effect due to the Rashba effective field $\vec{H}_{\text{Rashba}}$ due to the direct exchangelike interaction between the Rashba-induced spin accumulation and the magnetization.[3] The resulting torque has the symmetry of Eq. (4), and its magnitude τ_2 is given by approximately[21]

$$\tau_2^{\text{Rashba}} = \frac{\alpha_R j_c P}{\mu_B M_S}, \tag{7}$$

where μ_B is the Bohr magneton and P is the polarization of the carriers in the ferromagnetic layer; the Rashba parameter α_R is averaged over the magnetic film thickness. As already mentioned, an "indirect Rashba effect" has also been predicted and results in a torque of the SLT symmetry acting on the ferromagnetic layer.

In order to predict their influence, we have performed micromagnetic simulations of the DW motions induced by both torque symmetries. From now on, we consider that the Slonczewski torque (SLT) comes primarily from the SHE and/or IRE while FLT comes primarily from the direct Rashba effect. The effective fields associated with these torques can be defined conventionally,

$$\vec{H}_{\text{SLT}} = \tau_1 (\hat{m} \times \hat{\sigma}), \tag{8}$$

$$\vec{H}_{\text{FLT}} = \tau_2 \hat{\sigma}, \tag{9}$$

where τ_1 and τ_2 are can be related, respectively, to Eqs. (5) and (7) for the torques for the SHE and direct RE.

These two spin-torque symmetries have been predicted to strongly influence the DW dynamics.[22] Here we propose to investigate the conditions in terms of DW types and injection scheme [parallel geometry in Fig. 1(b) and perpendicular geometry in Fig. 1(c)] under which one of these spin-orbit torques is able to generate a very fast DW motion. The simulations are performed for long and thin (4 μm long and 3 nm thick) magnetic strips with different domain wall (DW) configurations: (i) in-plane magnetized NiFe layer with head-to-head (HTH) transverse walls, and (ii) perpendicularly magnetized Co/Ni multilayer with either Bloch or Néel DWs. For NiFe, we use the following magnetic parameters: $M_s = 800$ emu/cm^3, $A = 1.3 \times 10^{-6}$ erg/cm^2, $\alpha = 0.01$.[23] The width of the in-plane magnetized strip is chosen to be 100 nm. For simulating the case of perpendicularly magnetized layers, we use magnetic parameters corresponding to Co/Ni, i.e., $M_s = 650$ emu/cm^3, $A = 2 \times 10^{-6}$ erg/cm^2, $K_{\rm perp} = 3.3 \times 10^6$ erg/cm^3, $\alpha = 0.02$. In order to get the two DW structures, Bloch wall and Néel wall, we perform the simulations for two different widths: $w = 200$ nm for Bloch DW and $w = 50$ nm for Néel DW. For the parallel configuration [see Fig. 1(b)], the SO and the magnetic layers are adjacent on the whole length of the strip. For the perpendicular configuration [see Fig. 1(c)], we chose a strip width of 200 nm for the normal metal (NM) SO layer that is perpendicular to the magnetic strip. For the micromagnetic simulations, we start with an equilibrium state with a DW initially located in the middle of the magnetic strip for the parallel configuration and centered at the axis of the nonmagnetic SO strip for the perpendicular one. At time $t = 0$, a dc current is switched on, which in turn induces the SO torques acting on the DW. The magnitude of the torque and the field of the SHE are calculated using $\Phi_H = 0.2$. The field of the RE [see Eq. (9)] is taken to match that of the SHE, Eq. (8) (for $\hat{m} \perp \hat{\sigma}$). Therefore the magnitude of both the effective fields is about 3 Oe at $j_c = 10^6$ A/cm^2 for both NiFe and Co/Ni The micromagnetic simulations are performed by numerical integration of the Landau-Lifshitz-Gilbert (LLG) equation using our SpinPM micromagnetic package based on the fourth-order Runge-Kutta method with an adaptive time-step control for the time integration. The Oersted field contribution is not considered in the numerical simulations. Generally, it has the same symmetry as the Rashba field, with the only difference that the Rashba field can have different signs for different interfaces. However, the Oersted field and the effective fields associated to spin Hall and Rashba effects scale differently with the system size: At a given current density, the Oersted field contribution becomes negligible for small sizes, while the magnitude of the SHE and RE does not change.

We first investigate how the different SO effects are able to displace a DW in the parallel geometry, that is, the one commonly used in all the existing experimental studies.[4–8] In Fig. 2, we display the results for the different DW types and for a current density $J = 1$ MA/cm^2. The most remarkable result is that the only case in which a DW can be brought into a steady and fast motion (without any additional applied field) is for a Néel DW under the action of the torque due to SHE (red curve and inset in Fig. 2). The torque associated with RE only causes a small and reversible DW shift (blue curve in
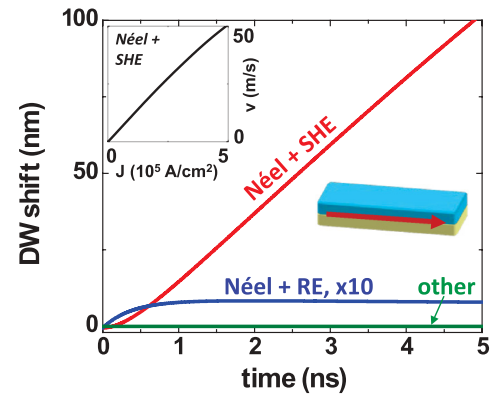

FIG. 2. (Color online) DW shift as a function of time under different possible SO torques in the parallel geometry. A steady motion is found for the case of a Néel wall excited by SHE (red curve) whereas for Néel wall with RE, the DW is only shifted (blue curve). Inset: Néel DW velocity induced by SHE vs current density in parallel geometry.

Fig. 2). For the two other DW types, none of the SO torques is able to induce substantial DW displacements (green curve in Fig. 2). This result can be simply explained if one considers the orientation of the effective field acting on the spins of the DW, which must be aligned with the magnetization of one of the adjacent domains to promote a steady motion.[18] For the parallel geometry, this prerequisite is fulfilled only for the Néel DW in a perpendicularly magnetized strip excited by the SHE: The effective field $H_{\rm SLT}$ is perpendicular to the plane at the center of the DW [see Eq. (4)]. In contrast, in the case of Bloch and HTH DWs, the directions of the SO spin accumulation and the magnetization direction at the DW center are parallel to each other along O_y and thus $H_{\rm SLT}$ vanishes. As for the Rashba effect, the direction of the effective field, $H_{\rm Rashba}$, according to Eq. (5), is given by the direction of the SO polarization $\hat{\sigma}$, which is along O_y, and therefore it is not along the domain direction for all three DW types.

Our results of steady and fast motion with Néel walls might appear rather surprising as Bloch DWs are expected in the existing experiments on the rather large Co/Pt or Co/Ni nanostrips in which large velocities have been obtained and ascribed to SHE or Rashba effects.[4–7] However, Haazen *et al.* have recently observed that a DW motion is induced by SHE in an asymmetric Pt/Co/Pt strip only when they apply a large field along O_x needed to favor Néel DWs.[8] It has been also shown that the Dzyaloshinski-Moriya (DM) interaction can be large at the interfaces with the materials having a large SO interaction. The DM interaction can result in stabilization of the Néel DW structure over the Bloch DW structure even for rather wide stripes.[24] Taking into account such DM coupling, Thiaville *et al.* recently demonstrated that it influences not only the static DW structure by favoring Néel DWs but also the DW dynamics, as it makes more difficult the transition to a Bloch DW structure, which can result in increasing the Walker breakdown and therefore allowing large DW velocities.[25] Therefore very large DW velocities observed recently in wide nanostrips made of perpendicularly magnetized Co/Pt and Co/Ni (Refs. 4–8) could be accounted for by the SHE or the indirect RE if one takes into account the additional stabilization
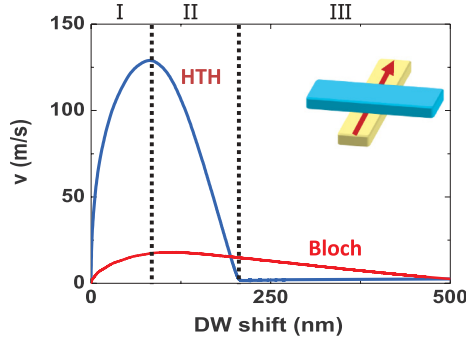
FIG. 3. (Color online) DW velocity as a function of DW position inside the F strip. Zero corresponds to the center of the intersection with the SO strip that is 200 nm wide. A steady motion is found for Bloch DW excited by SHE and for HTH DW excited by RE. Two regimes are identified, i.e., (I) the DW is inside the intersection area and a steady motion is obtained, and (II) the DW is outside the intersection and an inertial motion with decreasing velocity is found.

of the Néel DW by DM interactions. Another finding of our simulations is that the DW will move in opposite directions for opposite chiralities. However, it can be pointed out that DM interaction will induce the same chirality in all consecutive DW and thus motions in the same direction, which is the desired behavior for any type of DW-based memory devices.
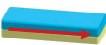
We now focus on the second geometry with the perpendicular configuration of the current [depicted in Fig. 1(c)]. In Fig. 3, we demonstrate that a DW steady motion is obtained for two combinations of DW type and SO effect: (i) a HTH DW excited by the direct Rashba effect and (ii) a Bloch DW excited by the SHE. We note that both the amplitude and the evolution of DW displacement with current depend on the DW type, with a largest value obtained for HTH DW driven by RE. These results can be explained, as in the case of parallel geometry, by looking at the directions of the effective fields associated with each SO torque type acting on the DW and compare them to magnetization directions in the adjacent domains. Since the polarization vector $\hat{\sigma}$ for the perpendicular geometry is along the O_x direction [see Fig. 1(c)], the Rashba field is also directed along O_x. As a consequence, H_{Rashba} is parallel to one of the magnetic domains for the case of an in-plane magnetized strip, explaining why Rashba-induced torque is able to put a HTH DW into motion in this perpendicular configuration (red curve in Fig. 3). Moreover, we find in this latter case that the direction of motion does not depend on the HTH DW chirality. As for the two other DW types, i.e., Bloch and Néel DWs, that are of some interest for memory applications, as the Rashba field H_{Rashba} is always perpendicular to the domains, we conclude that both DWs are only shifted on a very small distance, of the order of a few nm. If we now consider the action of SHE, its effective field H_{SLT} is along O_z for the in-plane magnetized strip and vanishes for the perpendicular geometry with the Néel DW, and thus no DW motion is expected for these cases. Finally, we find as shown in Fig. 3 that the SHE is able to move a Bloch DW in this geometry (the motion direction depends in this case on the DW chirality), again because H_{SLT} is perpendicular to the plane.

In the perpendicular geometry, the SO-induced torque acts on the DW only within the intersection of the magnetic strip and the SO current line. Therefore, there can be no steady-state

DW motion in this configuration. Instead, two regimes of the DW motion are observed (see Fig. 3). First, when the DW is within the intersection, it is accelerated by the SO field. The DW gets its maximum velocity just before leaving the intersection region. The second regime is the DW inertial motion after it leaves the intersection; now the DW is moving with the velocity decreasing linearly due to the damping. Eventually, the DW stops or it can start to move with a small velocity if it is attracted or repelled by the edges of the stripe. The maximum DW velocity as well as the DW total shift during this damped motion regime scale with the current density, as shown in Fig. 3. When the damping is sufficiently small and there are no pinning sites in the wire, we find that the DW can reach a few hundred m/s in velocities and thus can travel on a distance which is a few times larger than the length of the intersection region. Practical applications can be designed so that the magnetic strip has two or several intersections with the SO current lines, and a DW can be moved from one SO line to another by a current pulse flowing in the first SO line. In Table I, we summarize all our results of SO-driven DW motion in the different geometries.

Now we compare the efficiency of the DW motion by the SO-induced torques to the *conventional* spin-transfer-induced motion with in-plane currents injected in the magnetic wire (CIP case). The DW velocity of a Néel DW driven by SHE reaches about $\sim$20 m/s at a current density of $j = 0.2$ MA/cm^2 and increases linearly with j (see the inset of Fig. 2). The maximum velocity we find for the Bloch DW in the perpendicular configuration for the SHE is about 7 m/s for the same current. These values are close to the prediction of the one-dimensional (1D) model for a uniform external field $V_{\text{DW}} = \frac{\gamma H_{\text{eff}} \Delta}{\alpha}$, where Δ is the DW width, γ the gyromagnetic ratio, and α the damping. In our case, the effective field H_{eff} corresponds to H_{SHE}. In the *conventional* CIP case, one can use the same equation, where now H_{eff} is equal to an effective field associated with the nonadiabatic torque,[25] $H_{\text{IP}} = \frac{\hbar J_{\text{IP}} \beta P}{2e\Delta}$, where

TABLE I. Summary of the numerical results for the different DW types and injection geometry.

Injection geometry	Torque origin	DW type	Result
Parallel	SHE and/or IRE	Bloch	No motion
		Néel	Steady motion
		HTH	No motion
	Rashba	Bloch	No motion
		Néel	Shift
		HTH	No motion
Perpendicular	SHE and/or IRE	Bloch	Steady motion
		Néel	No motion
		HTH	No motion
	Rashba	Bloch	Shift
		Néel	No motion
		HTH	Steady motion

β is the nonadiabatic parameter. Comparing this expression to Eqs. (5) and (6), which give the amplitude of the SO fields for either case, i.e., $H_{SO} = \frac{\hbar J_{IP} \Phi_{SO}}{2ed}$, we easily find that the ratio of the SO field and the field in the *conventional* case is equal to the ratio of the DW velocities, $\frac{v_{SO}}{v_{CIP}} = \frac{H_{SO}}{H_{CIP}} = \frac{\Phi_{SO}}{\beta P} \frac{\Delta}{d}$. Thus we conclude that SO-driven DW motion can be faster than in the *conventional* case by at least a factor of 10 as the nonadiabatic term β is always about a few percent[27] and the ratio of the DW width over film thickness Δ/d is never lower than unity.

In conclusion, we have performed a comprehensive numerical study to identify the best conditions of domain-wall type, current direction, and spin-orbit induced transfer torque, SHE or Rashba, promoting a fast current-induced DW motion. As this can be equally expected from symmetry arguments, we find that DWs can be moved using SO effects in two cases: (1) for a Néel DW by the torque induced by SHE for the case of a perpendicularly magnetized strip and a nonmagnetic stripe parallel to the magnetic one, and (2) for a Bloch wall (out-of-plane magnetization) by SHE and (3) head-to-head DW (in-plane magnetization) by the Rashba effect with a current flowing in a nonmagnetic strip perpendicular to the magnetic one. Moreover, we find an improved efficiency of SO torques compared to the conventional CIP DW motion, making the SO effects very promising to be used in the next generation of DW-based spintronic devices.

*Corresponding author: vincent.cros@thalesgroup.com

[1] M. I. Dyakonov and V. I. Perel, JETP Lett. **13**, 467 (1971); Phys. Lett. A **35**, 459 (1971).

[2] Yu. A. Bychkov and E. I. Rashba, J. Exp. Theor. Phys. Lett. **39**, 78 (1984); G. Dresselhaus, Phys. Rev. **100**, 580 (1955).

[3] A. Manchon and S. Zhang, Phys. Rev. B **79**, 094422 (2009); K. Obata and G. Tatara, *ibid.* **77**, 214429 (2008); O. Krupin, G. Bihlmayer, K. Starke, S. Gorovikov, J. E. Prieto, K. Döbrich, S. Blügel, and G. Kaindl, *ibid.* **71**, 201403(R) (2005).

[4] I. M. Miron, G. Gaudin, S. Auffret, B. Rodmacq, A. Schuhl, S. Pizzini, J. Vogel, and P. Gambardella, Nat. Mater. **9**, 230 (2010).

[5] I. M. Miron, T. Moore, H. Szambolics, L. D. Buda-Prejbeanu, S. Auffret, B. Rodmacq, S. Pizzini, J. Vogel, M. Bonfim, A. Schuhl, and G. Gaudin, Nat. Mater. **10**, 419 (2011).

[6] L. Liu, C. F. Pai, Y. Li, H. W. Tseng, D. C. Ralph, and R. A. Buhrman, Science **336**, 555 (2012).

[7] S. Emori, D. C. Bono, and G. S. D. Beach, Appl. Phys. Lett. **101**, 042405 (2012).

[8] P. P. J. Haazen, E. Murè, J. H. Franken, R. Lavrijsen, H. J. M. Swagten, and B. Koopmans, arXiv:1209.2320.

[9] L. Liu, O. J. Lee, T. J. Gudmundsen, D. C. Ralph, and R. A. Buhrman, Phys. Rev. Lett. **109**, 096602 (2012).

[10] V. E. Demidov, S. Urazhdin, H. Ulrichs, V. Tiberkevich, A. Slavin, D. Baither, G. Schmitz, and S. O. Demokritov, Nature Materials **11**, 1029 (2012).

[11] T. Kimura, Y. Otani, T. Sato, S. Takahashi, and S. Maekawa, Phys. Rev. Lett. **98**, 156601 (2007); L. Vila, T. Kimura, and Y. C. Otani, *ibid.* **99**, 226604 (2007).

[12] Y. K. Kato, R. C. Myers, A. C. Gossard, and D. D. Awschalom, Science **306**, 1910 (2004); J. Wunderlich, B. Kaestner, J. Sinova, and T. Jungwirth, Phys. Rev. Lett. **94**, 047204 (2005).

[13] Y. Niimi, Y. Kawanishi, D. H. Wei, C. Deranlot, H. X. Yang, M. Chshiev, T. Valet, A. Fert, and Y. Otani, Phys. Rev. Lett. **109**, 156602 (2012).

[14] C. F. Pai, L. Liu, Y. Li, H. W. Tseng, D. C. Ralph, and R. A. Buhrman, Appl. Phys. Lett. **101**, 122404 (2012).

[15] C. R. Ast, J. Henk, A. Ernst, L. Moreschini, M. C. Falub, D. Pacilé, P. Bruno, K. Kern, and M. Grioni, Phys. Rev. Lett. **98**, 186807 (2007); F. Meier, H. Dil, J. Lobo-Checa, L. Patthey, and J. Osterwalder, Phys. Rev. B **77**, 165431 (2008); I. Gierz, F. Meier, J. H. Dil, K. Kern, and C. R. Ast, *ibid.* **83**, 195122 (2011).

[16] X. Wang and A. Manchon, Phys. Rev. Lett. **108**, 117201 (2012); A. Manchon, arXiv:1204.4869.

[17] D. A. Pesin and A. H. MacDonald, Phys. Rev. B **86**, 014416 (2012); E. van der Bijl and R. A. Duine, *ibid.* **86**, 094406 (2012).

[18] A. V. Khvalkovskiy, K. A. Zvezdin, Ya. V. Gorbunov, V. Cros, J. Grollier, A. Fert, and A. K. Zvezdin, Phys. Rev. Lett. **102**, 067206 (2009).

[19] M. D. Stiles and J. Miltat, in *Spin Dynamics in Confined Magnetic Structures III*, edited by B. Hillebrands and A. Thiaville, Topics in Applied Physics Vol. 101 (Springer, Berlin, 2006), pp. 225–308; A. Manchon, arXiv:1207.5231.

[20] A. Chanthbouala, R. Matsumoto, J. Grollier, V. Cros, A. Anane, A. Fert, A. V. Khvalkovskiy, K. A. Zvezdin, K. Nishimura, Y. Nagamine, H. Maehara, K. Tsunekawa, A. Fukushima, and S. Yuasa, Nat. Phys. **7**, 626 (2011).

[21] A. Manchon and S. Zhang, Phys. Rev. B **78**, 212405 (2008).

[22] S.-M. Seo, K.-W. Kim, J. Ryu, H.-W. Lee, and K.-J. Lee, Appl. Phys. Lett. **101**, 022405 (2012); K.-W. Kim, S.-M. Seo, J. Ryu, K.-J. Lee, and H.-W. Lee, Phys. Rev. B **85**, 180404 (R) (2012).

[23] S. Mangin, D. Ravelosona, J. A. Katine, M. J. Carey, B. D. Terris, and E. E. Fullerton, Nat. Mater. **5**, 210 (2006); D. Ravelosona (private communication).

[24] M. Heide, G. Bihlmayer, and S. Blügel, Phys. Rev. B **78**, 140403(R) (2008).

[25] A. Thiaville, S. Rohart, E. Jué, V. Cros, and A. Fert, Eur. Phys. Lett. **100**, 57002 (2012).

[26] A. Thiaville, Y. Nakatani, J. Miltat, and Y. Suzuki, Eur. Phys. Lett. **69**, 990 (2005).

[27] O. Boulle, G. Malinowski, and M. Kläui, Mater. Sci. Eng. R **72**, 159 (2011).